Supporting Information

Photoswitching Mechanism of Cyanine Dyes

Graham T. Dempsey, Mark Bates, Walter E. Kowtoniuk, David R. Liu, Roger Y. Tsien, and Xiaowei Zhuang

Supporting Information Contents:

Experimental Procedures

Figure S1: Kinetics of thermal and UV light-induced reactivation of Cy5 from the dark state.

Figure S2: Molecular structures of the cyanine dyes and thiols used in this study.

Figure S3: Negative mode MS/MS of Cy5-COOH and its dark state βME conjugate.

Figure S4: Positive mode MS of Cy5-COOH and its dark state βME conjugate.

Figure S5: Positive mode MS/MS and peak assignment of the Cy5-COOH starting material.

Figure S6: Positive mode MS/MS and peak assignment of the Cy5-COOH-βME conjugate.

Figure S7: Positive mode MS/MS of Cy5-diethyl and its βME conjugate.

Figure S8: Negative mode MS of the dark state of Cy5-COOH formed in the presence of L-Cys-ME.

Figure S9: Effect of radical quencher on Cy5 switching kinetics.

Table S1: Predicted and measured masses of cyanine dyes and their corresponding dark state products.

Experimental Procedures:

Ensemble photoconversion. MiliQ water and a 1M Tris pH 8.0 solution were Ar bubbled for 10 min, degassed for 15 min, followed by additional Ar bubbling for 10 min and overnight degassing before being used for subsequent sample preparation. To generate the carboxylic acid version of Cy5-NHS and Cy7-NHS (GE Healthcare), the dyes were mixed with water to ~500 μM concentration and vortexed vigorously. Cy5-diethyl (a gift from Marcel Bruchez at Carnegie Mellon University) was dissolved in water to the same concentration and all dye stocks were used without further purification. For photoconversion of the cyanine dyes, the solution conditions were adjusted to ensure optimal switching and stable pH. Specifically, a solution of 4 – 5 μM dye was prepared with either 143 mM βME (Fluka) in 50 mM Tris pH 8.0, 10 mM MEA (Fluka) in water, or 100 mM L-cysteine methyl ester (Sigma) in 500 mM Tris pH 8.0. The sample was loaded into a 100 μL cuvette and sealed with parafilm. To switch the cyanine dyes to the dark state, the cuvette was illuminated with 300 mW of a defocused 647 nm laser line of an Ar-Kr Innova 70C Spectrum laser (Coherent) for 5 min. For MS/MS analysis, 200 – 250 μM Cy5-COOH or Cy5-diethyl was photoconverted as described above, but in the presence of 100 mM $NaHCO_3/Na_2CO_3$ pH 10.5. Reactivation was carried out by passing light from a mercury lamp (Olympus) through a band-pass emission filter (325 nm/30 nm for Cy5 and 350 nm/50 nm for Cy7, Chroma) before focusing onto the cuvette. The samples used for MS analysis were illuminated for 5 min for Cy5 samples and 1 – 2 min for Cy7 samples. For reactivation kinetics measurements, the Cy5 dark material was either exposed to UV light for different time intervals or allowed to recover at room temperature in the dark. Recovery of Cy5 absorption in the latter case resulted from thermal reactivation from the dark state, as evidenced by the fact that freezing the sample or storing it at 4^oC following red laser illumination greatly reduced the rate of

recovery. To measure the absorption spectra of cyanine dyes following red or UV exposure, a UV-Visible spectrophotometer was used (Beckman DU800). Each Cy5 spectrum was corrected by subtracting the background absorbance at 750 nm. Cy7 spectra were corrected for the absorbance at 875 nm.

Single-molecule imaging. Single-stranded, 43-base pair DNA constructs (purchased PAGE-purified from Operon) were labeled, annealed, and purified as described previously.[1,2] One strand (sequence 5'-ATG CTA ACG TAT GCA ATG GTA ATG ATA CTG A[AmC2-dT]C GTA ATA ACG C-3') was labeled with Cy5-NHS (GE Healthcare) through an internal dT modified by an amine group at the end of a 2-carbon linker (labeled as AmC2-dT). A complimentary strand with a biotin linker (sequence 5'-GCG T[AmC2-dT]A TTA CGA TCA GTA TCA TTA CCA TTG CAT ACG TTA GCA T-3'-Biotin) was either labeled with Cy3-NHS (GE Healthcare) or left unlabeled, and then annealed to the Cy5-labeled strand. Experiments in Figure 1A-C insets were performed with the Cy5-labeled DNA without a Cy3 label, while experiments in Figure 1D-E were performed with Cy5 attached to one strand of the double-stranded DNA construct and Cy3 attached to the complementary strand.

To demonstrate red-illumination induced conversion to the dark state and UV-illumination induced recovery (experiments shown in Figure 1A-C insets), Cy5-labeled DNA was then immobilized to a glass surface via a biotin-streptavidin linkage, as described previously[1], before imaging via total internal reflection fluorescence (TIRF) microscopy. Prior to imaging, a solution of 50 mM Tris pH 8.0, 10 mM NaCl, 10% (w/v) glucose, 0.5 mg/mL glucose oxidase (Sigma), 40 μg/mL catalase (Roche Applied Science), and 143mM βME (Fluka) was added to the chamber. The mixture of glucose, glucose oxidase, and catalase served as an oxygen scavenger system to prevent photobleaching of the dye molecules. Dye-labeled DNA was

imaged on an Olympus IX-71 inverted objective-type TIRF microscope. Cy5 on the DNA was illuminated by the 647 nm laser line (Coherent), which served the dual purposes of exciting fluorescence from Cy5 and switching of the Cy5 to the dark state. A long-pass dichroic mirror (Z660DCXRU, Chroma) was used to reflect the laser light toward the sample before passing through a 100x, NA 1.4 oil immersion objective (UPlanSApo, Olympus). Fluorescence was collected through a band-pass emission filter (HQ700/75, Chroma) and imaged onto a EMCCD camera (Andor Ixon DV897DCS-BV). For reactivation, a brief (~5 – 10 s) exposure from a Hg lamp source (Olympus) was used to illuminate the sample by passing through a band-pass excitation filter (387 nm/11 nm, Semrock) and reflecting off of a dichroic mirror (FF409-Di02, Semrock) before passing through the objective to the sample.

Single molecule kinetic measurements. For measurements of the photoswitching kinetics (Figure 1D, E), DNA labeled with both Cy3 and Cy5 was prepared and immobilized onto quartz slides as described above. The presence of a Cy3 label ensured that Cy5 can be reactivated efficiently in response to 532 nm light.[1,2] The appropriate buffer was also added to the solution used prior to imaging in order to maintain a particular pH. For pH values between pH 5.7 – 6.7, 7.5 – 8.6, and 8.8 – 9.8, PIPES, Tris, and carbonate buffers were used, respectively, at 50 mM concentration. The βME concentration in the final imaging solution was also varied. For imaging, an Olympus IX-71 microscope was configured for prism-type TIRF, as described previously.[2] A 633 nm HeNe laser (Melles Griot) was used for excitation of Cy5 and switching it to the dark state. For reactivation, a 532 nm diode-pumped solid state laser (Crystalaser) was used. The Cy5 fluorescence was collected by a 60x, NA 1.2 water immersion objective (Olympus) and passed through a long-pass emission filter (HQ645LP, Chroma). The final image was magnified to ~100x by a 1.6x tube lens before being collected by the EMCCD camera. To

measure the rate of switching to the dark state (k_{off}), the Cy3-Cy5-DNA sample was illuminated with 633 nm laser light to switch the Cy5 molecules to the dark state. The rate was determined by counting the number of molecules in the field of view for each frame and then fitting the distribution to a single exponential function. The measured rates were normalized by the laser intensity used, as we have shown previously that the switching rate constant scales linearly with the excitation intensity.[1,2] For each condition, following red excitation, a brief exposure to ~5 W/cm^2 of 532 nm laser light was used to reactivate nearly all of the molecules that were switched to the dark state. The fraction that recovered was used to ensure that the rate of switching off was predominantly due to switching to the dark state and not from photobleaching.

Analysis of the photoconversion kinetics. For the photoconversion kinetic scheme as shown in Scheme 1, we assume rapid and reversible formation of the encounter complex Cy5•RS$^-$. At equilibrium we can write:

$$(1) \quad [Cy5 \cdot RS^-] = \frac{[Cy5][RS^-]}{K_d}$$

where K_d is the dissociation constant of the Cy5•RS$^-$ encounter complex. The probability that a given Cy5 molecule will be in the encounter complex can be expressed as:

$$(2) \quad F_{complex} = \frac{[Cy5 \cdot RS^-]}{[Cy5 \cdot RS^-] + [Cy5]}$$

Combining equations (1) and (2), this probability can be further expressed as:

$$(3) \quad F_{complex} = \frac{F_{RS^-}[\beta ME]/K_d}{F_{RS^-}[\beta ME]/K_d + 1}$$

where F_{RS^-} = [RS$^-$] / [βME] is the fraction of the βME that is deprotonated. Under our excitation conditions, the fraction of Cy5 molecules in the excited state is much lower than those in the ground state at any given time ($\sigma I << k_f$). The overall rate constant for switching to the dark state

(k_{off}) is the product of: (*i*) the fraction of the Cy5 molecules that are in the encounter complex ($F_{complex}$), (*ii*) the rate constant for exciting Cy5 (σI), and (*iii*) the quantum yield for the formation of the dark state product from the excited state complex (k_0 / (k_0 + k_f)). Therefore, k_{off} can be expressed as:

$$(4) \quad k_{off} = \frac{\sigma I k_0}{k_0 + k_f} \cdot \frac{F_{RS^-}[\beta ME]/K_d}{F_{RS^-}[\beta ME]/K_d + 1}$$

where the excitation cross-section σ can be expressed in units of cm^2 and the excitation intensity I in units of photon·$cm^{-2}s^{-1}$. A two parameter fit was performed with the above expression to extract the values of F_{RS^-}/K_d and σk_0 / (k_0 + k_f) from our switching kinetics measurements at different concentrations of βME (k_{off} / I vs. [βME], Figure 1D). From this fit, we deduced the saturation value of k_{off} / I, namely σk_0 / (k_0 + k_f), to be 0.004 $s^{-1}W^{-1}cm^2$ or 1.3×10^{-21} $photon^{-1}cm^2$. Assuming that the extinction coefficient of the Cy5•RS^- encounter complex is the same as that of a free Cy5, ~1.9×10^5 $M^{-1}cm^{-1}$ (at 633 nm), the cross-section σ of a Cy5•RS^- complex is then 7.2×10^{-16} cm^2. The quantum yield of photoconversion, k_0 / (k_0 + k_f), is then derived to be ~2×10^{-6}.

To relate the fraction of deprotonated thiol derived from these fits to the solution pH, we then repeated the kinetic measurements for a range of pH values. By the Henderson-Hasselbalch equation, the freely ionized thiol can then be written as:

$$(5) \quad {F_{RS^-}}/{K_d} = \frac{1/K_d}{1 + 10^{pK_a - pH}}$$

Experimentally derived F_{RS^-} / K_d values from the k_{off} / I vs. [βME] curves were fit to Equation 5 to extract the pK_a (9.74 ± 0.05) of βME and the K_d (22 ± 2 μM) for the encounter complex (Figure 1E).

We also considered an alternative kinetic scheme in which excitation of the Cy5 must precede formation of the encounter complex with the thiol anion (See Scheme 1*).

Scheme 1*.

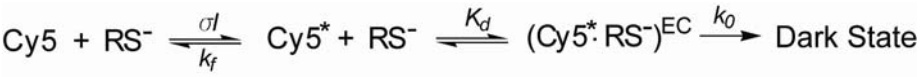

The problem with this scheme is that the excited state of Cy5 only lasts ~1 ns ($k_f \sim 10^9$ s^{-1}), not nearly long enough to engage in reversible equilibrium binding to a thiol anion to support an equilibrium dissociation constant of K_d ~22 μM, given that diffusion limits bimolecular rate constants to ~10^{10} $M^{-1}s^{-1}$. Another way to understand this argument is that even the most effective dynamic fluorescence quenchers, which diffuse as fast as O_2 and react with every excited state that they encounter, require concentrations of several tens of millimolar before their effectiveness begins to saturate. Since the observed effect of thiol anions begins to saturate at about 3 orders of magnitude lower concentration (Figure 1D), we do not consider Scheme 1* feasible. However, a scheme that allows the excitation of Cy5 to occur either before or after the formation of the encounter complex (See Scheme 1**) cannot be ruled out.

Scheme 1.**

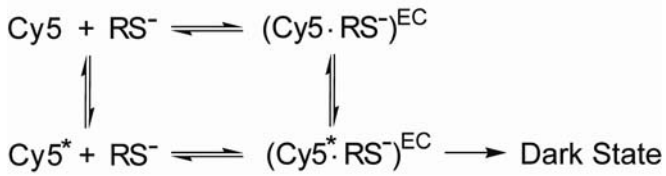

As both the formation rate of the dark state from the encounter complex and the excitation rate of the dye are much smaller than the de-excitation rate, Scheme 1** gives similar results to that of Scheme 1.

ESI-LC/MS and Tandem MS Analysis of Cyanine Dyes and their Dark State Products. Negative mode LC/MS was performed using a Waters Aquity UPLC Q-TOF Premier instrument with an Aquity UPLC BEH C18 column (1.7 μm, 2.1 mm x 100 mm, Waters). Mobile phase A was 0.1% aqueous ammonium formate, and mobile phase B was methanol. The flow rate was a constant 0.300 mL/min and the mobile phase composition was as follows: 0% B for 3 min; linear increase to 100% B over 17 min; maintain at 100% B for 2 min before returning linearly to 0% B over 1 min. Electrospray ionization (ESI) was used with a capillary voltage of 3.5 kV, sampling cone voltage of 40.0 kV, and collision voltage of 1.0 V. The drying gas temperature was 300 ºC, the drying gas flow rate was 800 L/hour, the source temperature was 150 ºC, and the detector was operated in negative ion mode. For each sample, 15 μL of the reaction mixture was injected without any additional workup. For positive mode LC/MS analysis, the following changes were made: mobile phase A was 0.1% formic acid, the capillary voltage was 3.4 kV, sampling cone voltage was 30.0 kV, collision voltage of 1.0 V, and the detector was operated in positive mode. The dark state adduct and the starting material were detected as distinguishable peaks in the chromatogram, and mass spectra were subsequently determined by integrating the chromatogram for the starting, dark state, and UV reactivated material over the same region encompassing both peaks. For the reported *m/z* values, the peaks were fit to determine the centroid.

LC/MS/MS experiments were performed using the same instrument, LC gradient, and MS parameters as described above for the respective ion detection mode, except the collision voltage was 40.0 V. The LM resolution was 4.7, and the HM resolution was 15. Fragment peak values were evaluated by fitting to determine the centroid.

Analysis of the Regiochemistry of Thiol Attachment to Cy5 by MS/MS. To determine the regiochemistry of thiol addition, we considered the possible attachment points of the thiol to the

Cy5 molecule. Given that the thiol is unlikely to be a sufficiently strong nucleophile under our reaction conditions to disrupt the aromatic rings of Cy5, the five carbons along the polymethine bridge and the two imine carbons that connect the bridge to the indolenine rings are the most plausible attachment sites. Considering the symmetric core Cy5 structure, four unique regioisomers may be formed with the thiol attached to the imine carbon (C0), or the first (C1), second (C2), or third (C3) carbon of the polymethine bridge (See Scheme 2* below), although two of them (addition to C1 or C3) will be highly unlikely as they violate charge conservation by requiring one indole nitrogen (highlighted in blue with an asterisk) to receive excess electrons. C4, C5, and C6 are equivalent to C2, C1, and C0, respectively, and will not be considered separately.

Scheme 2*

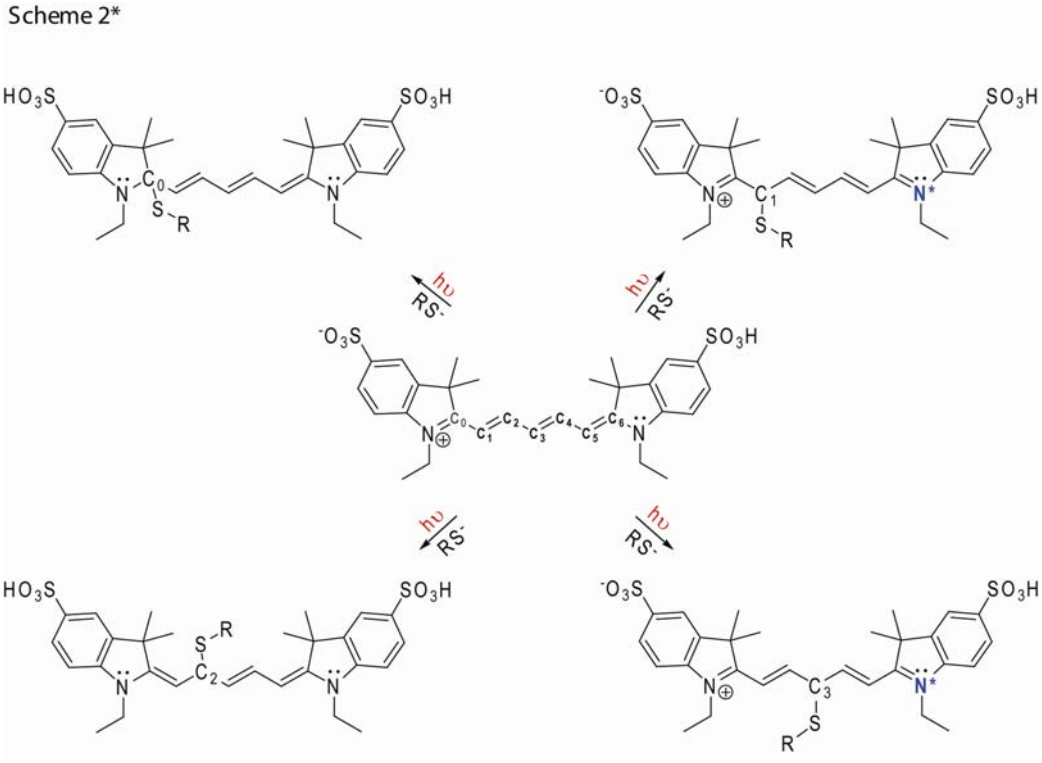

To experimentally probe the regiochemistry of the dark state Cy5-βME conjugate, we performed MS/MS analysis to determine the most likely attachment site from the fragmentation

patterns. While negative ion mode LC/MS provided direct evidence that the dark state was a Cy5-thiol adduct, the negative mode LC/MS/MS analysis of the dark state Cy5-βME conjugate suggested immediate loss of the thiol moiety from the parent ion prior to the generation of any other anionic fragment (Figure S3), preventing assignment of the thiol attachment site. We therefore conducted positive ion mode LC/MS/MS analysis to further investigate the regiochemistry. Under positive mode ionization conditions, we observed oxidation of the Cy5-βME conjugate, resulting in a product ion of $[M+H-H_2]^+$ $|m/z|$ = 733.24 (Figure S4B, S4C). Oxidation of analytes during electrospray ionization is commonly observed, especially when it is difficult to generate the properly charged ions during MS ionization.[3-6] In the case of the Cy5-thiol adduct as proposed in Scheme 2*, it is indeed much easier to generate a negatively charged ion by loss of a proton at one of the sulfonate groups than to generate a positively charged ion. Such oxidation of the Cy5-βME conjugate during MS ionization was further confirmed by the fragmentation pattern observed with LC/MS/MS (see, for example, comparison of the peak at 657.24 of the starting material in Figure S5 with the peak at 656.23 for the oxidized Cy5-βME conjugate after loss of the thiol during fragmentation in Figure S6). Such oxidation-induced shifts were not observed in negative ionization mode. Spectroscopic evidence also suggests that the structure observed in the positive mode MS is unlikely to be the dark state product from photoconversion, but rather the oxidized structure formed during MS ionization. During the photocoversion process, the original absorption peak at 650 nm diminished and a new absorption peak at approximately half of the wavelength (~310 nm) appeared (Figure 1B), indicating disruption of the conjugated π electron system. This spectroscopic change is consistent with the proposed unoxidized form of the Cy5-βME adduct, but not with the proposed oxidized form where the conjugated π electron system is restored (Figure S4C).

Despite the oxidation, the positive mode MS/MS spectrum of the Cy5-βME conjugate reveals a number of additional peaks that were not observed for the starting Cy5-COOH material (compare Figure S6B with Figure S6A or Figure S5), allowing us to probe the regiochemistry of the thiol addition. Several of these peaks ($|m/z|$ = 328.08, 378.11, 394.11, 464.13, 482.18, 685.18, 703.19, 718.22, and 733.24) showed an additional 4-Dalton shift when deuterated βME (d_4-βME) was used to generate the dark state product (compare Figure S6B with Figure S6C), corresponding to fragments with the full thiol group attached and facilitating peak assignment. The fragment assignment of all peaks observed for the starting Cy5-COOH material and all of the additional peaks observed for the Cy5-COOH-βME conjugate are shown in Figure S5 and S6, respectively. We have also performed MS/MS analysis of the dark state product from another Cy5 dye, the Cy5-diethyl-βME conjugate, the MS/MS spectrum and fragment assignment of which are shown in Figure S7.

With these fragmentation patterns, we first considered the possibility of the imine carbons as the thiol attachment site. We observed fragments which are consistent with a progressively shorter polymethine bridge and ultimately fragments consistent with the bridge completely removed (e.g. the peaks at 352.12, 338.11, 266.08, and 252.07 in Figure S5. The same four peaks were observed in Figure S6B. The 266.08 and 252.07 peaks were also observed in Figure S7B). However, we never observed fragments consistent with the bridge completely removed but the thiol still present in the MS/MS spectrum of the Cy5-COOH-βME or Cy5-diethyl-βME conjugate (Figure S6 and S7), suggesting that the imine carbons (C0 and C6), and the aromatic rings, are unlikely the attachment site for the thiol. This notion is also consistent with the significant steric hindrance at the C0 and C6 positions. Furthermore, thiol addition at the imine carbon would not allow further oxidation of that carbon, and the consequent loss of two protons

during ionization, as we have observed in the positive ion mode MS (Figure S4C). Therefore, we exclude these positions and considered the carbon atoms on the polymethine bridge as the remaining plausible thiol attachment sites.

Attachment of the thiol to the polymethine bridge is also consistent with the observation of the two peaks at $|m/z|$ = 378.11 and 482.18 in the MS/MS spectrum of the Cy5-COOH-βME conjugate (Figure S6B). The asymmetric structure of Cy5-COOH with the long aliphatic linker attached to only one of the indole nitrogen atoms allowed us to assign these two peaks: A break at the C1 carbon bond would give the 482.18 peak, in which the indolenine ring with the long aliphatic linker is now included along with the polymethine bridge and bound thiol; a break at the C5 carbon would result in the peak at 378.11, which consists of the indolenine ring with the short ethyl group along with the polymethine bridge and bound thiol. The inclusion of the thiol on both fragments, of which the only common part is the polymethine bridge, is consistent with attachment of the thiol to the bridge.

Next, we considered individual carbon atoms (C1, C2, and C3) on the polymethine bridge. Examination of the reaction Scheme 2* indicates that addition of the thiol at either C1 or C3 would violate charge conservation by requiring one indole nitrogen (highlighted in blue with an asterisk in Scheme 2*) to receive excess electrons following electronic rearrangement. In addition, the peaks observed at $|m/z|$ = 328.08 and 328.07 in the MS/MS spectra of the Cy5-COOH-βME and Cy5-diethyl-βME conjugates, respectively (Figures S6, S7), are inconsistent with the C3 position as the attachment point, as the C3 carbon was removed from the fragment but the thiol group remained attached. Therefore, we conclude that the C2 position is the most plausible attachment site for the thiol group as shown in Scheme 2 of the text, although we cannot formally exclude other potential attachments sites.

Supporting Figures:

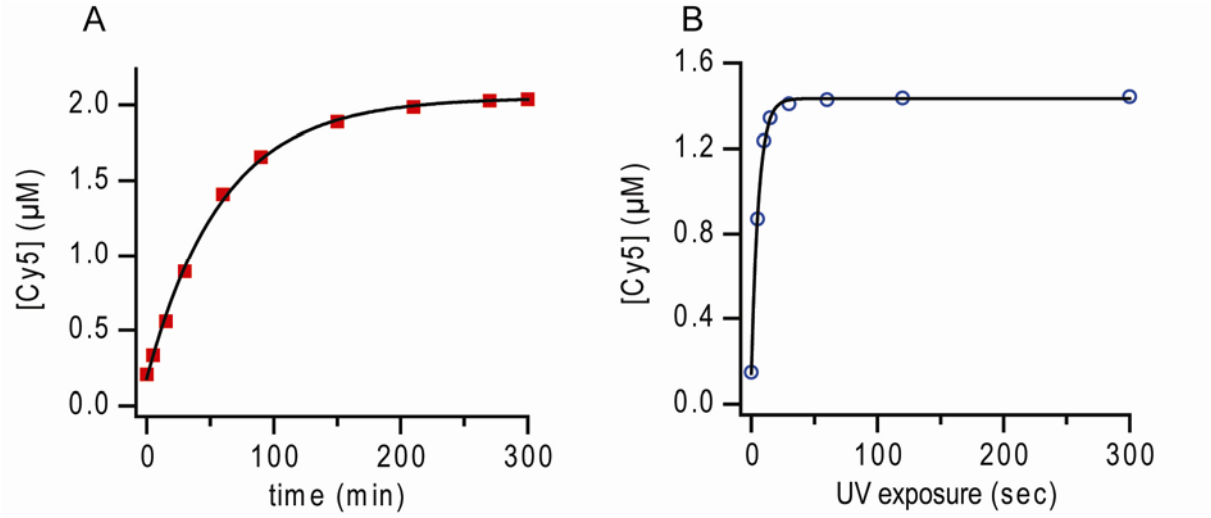

Figure S1. Kinetics of thermal and UV light-induced reactivation of Cy5-COOH from the dark state. A solution of Cy5-COOH was illuminated with a red laser in the presence of βME. The photoconversion product was either left to recover in the dark at room temperature (A) or exposed to UV light (B) for various amount of time. The amount of recovered Cy5 was measured by UV-Vis absorption at 650 nm and plotted as a function of time. The data points were fit with a single exponential function to extract rate constants of 0.017 min^{-1} and 0.175 sec^{-1} for (A) and (B), respectively. The presence of UV light thus enhanced the rate of recovery by 3 orders of magnitude. By keeping the dark state at 4°C or lower without UV illumination, the recovery was further slowed down substantially (data not shown), indicative of a thermal process accounting for the spontaneous recovery in the absence of UV illumination. MS analysis of the thermally recovered material resulted in the expected Cy5 mass peak and a disappearance of the dark state peak in both the chromatogram and mass spectrum.

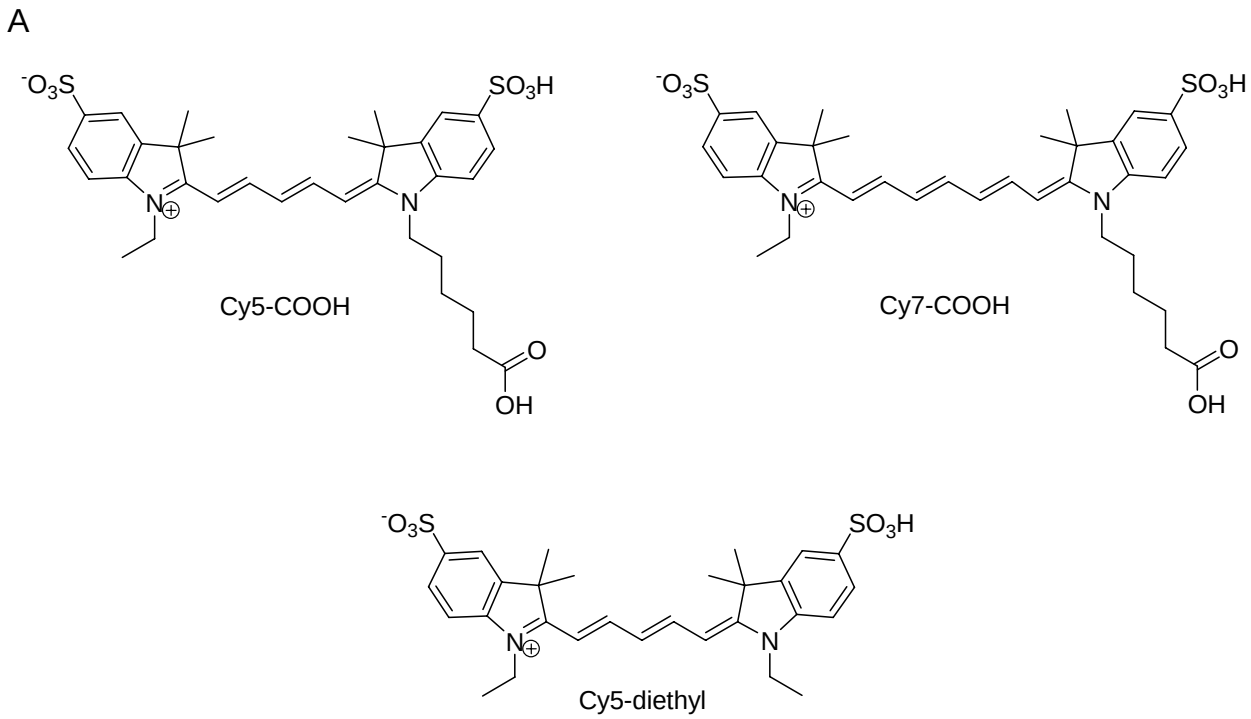

Figure S2. Molecular structures of the cyanine dyes (A) and thiol-containing compounds (B) used in this study.

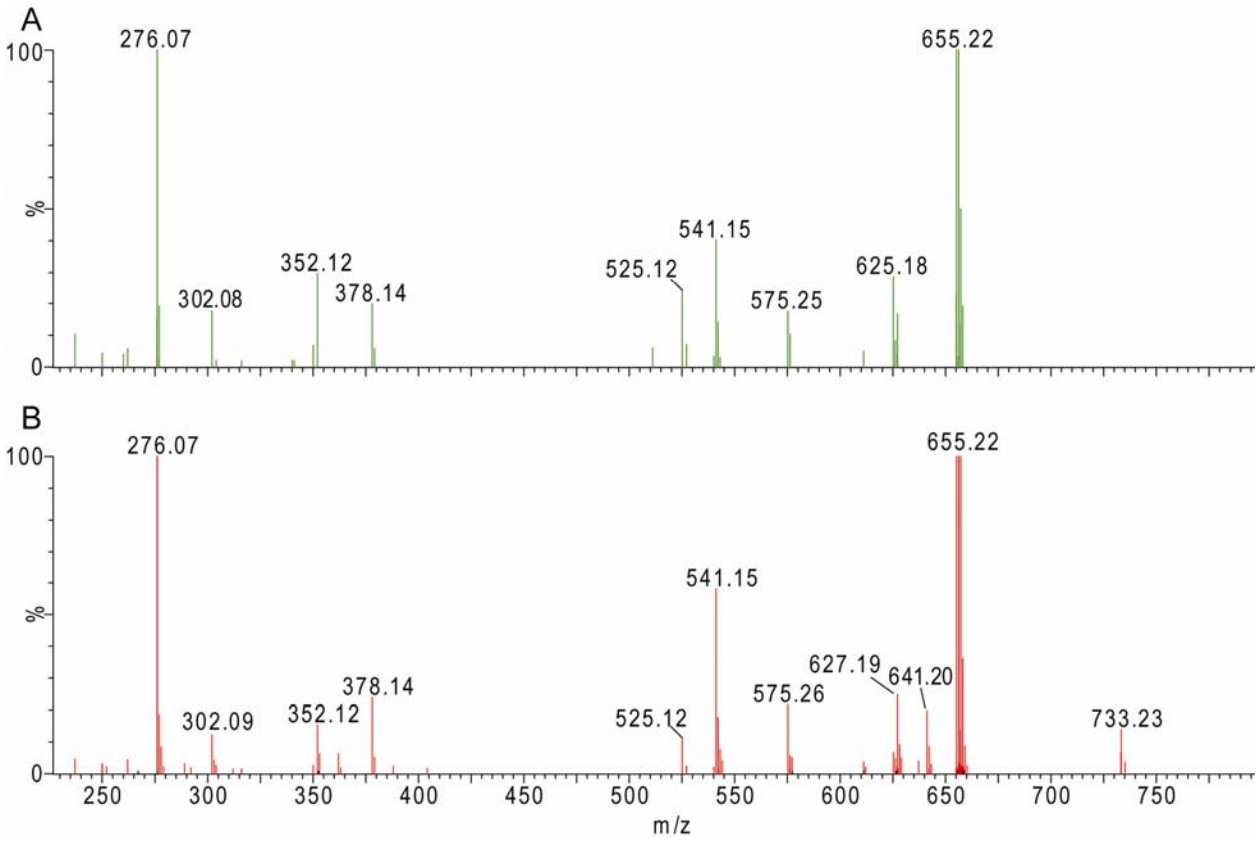

Figure S3. Negative mode MS/MS of Cy5-COOH and its dark state βME conjugate. (A) A Cy5-COOH/βME mixture was subjected to LC-MS, and the peak at 655.22 was further analyzed by MS/MS fragmentation. (B) The same Cy5-COOH/βME mixture was exposed to red laser illumination and then analyzed as in (A), now selecting the dark state adduct peak at 733.23 for MS/MS fragmentation analysis. The observed fragmentation patterns in both cases show no major difference, with the exception of the expected parent ion peak at 733.23 and the peaks at 627.19 and 641.20 in panel (B). These results indicate that the thiol group was the first portion of the dark state product to be removed during MS/MS, preventing the determination of regiochemistry of thiol attachment using negative mode MS/MS.

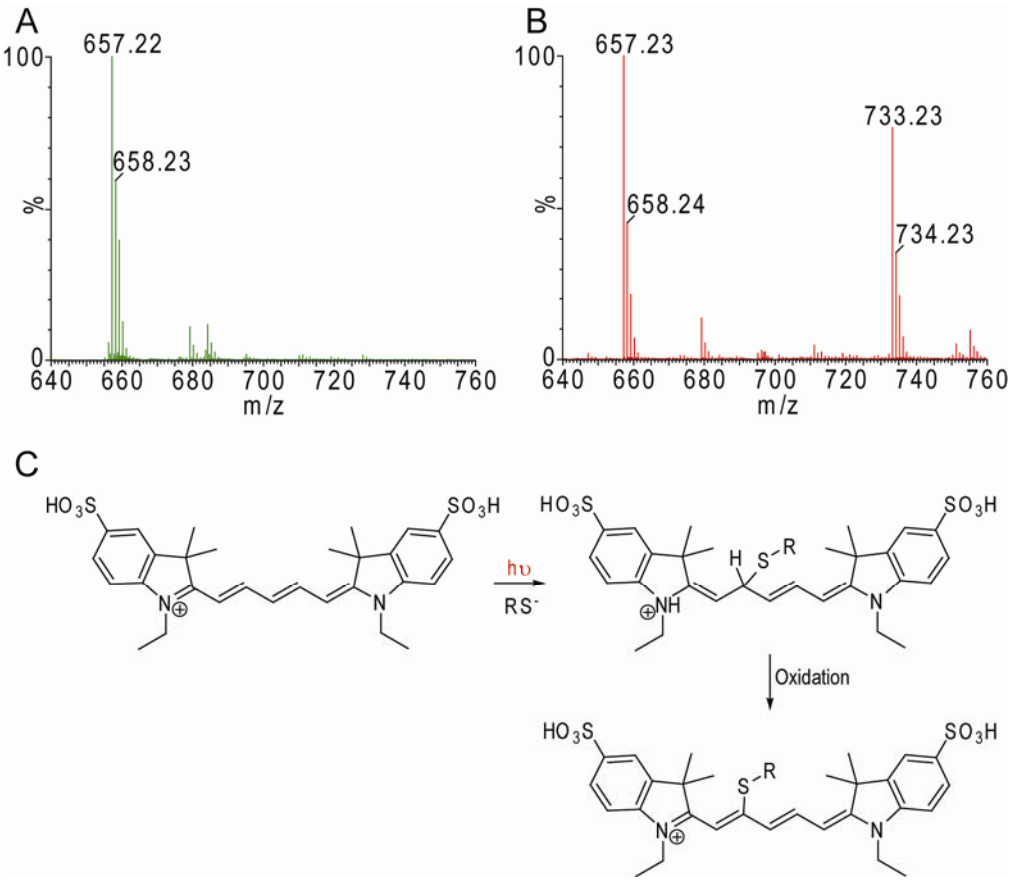

Figure S4. Positive mode MS of Cy5-COOH and its dark state βME conjugate. The panels show the cyanine dye-thiol mixture before (A) and after (B) red laser illumination, as well as a possible oxidation pathway resulting from positive mode MS (C). In the spectra, the peak that appears at $[M]^+$ $|m/z| = 657.22$ corresponds to $[Cy5\text{-}COOH]^+$. After red illumination, a new peak emerges as a singly charged species at $|m/z| = 733.23$. The predicted mass of the dark state in positive mode is $[M+H]^+$ $|m/z| = 735.24$. However, due to oxidation during MS ionization, as depicted in (C), the dark state loses two protons, resulting in the $[M+H-2H]^+$ $|m/z| = 733.23$ peak.

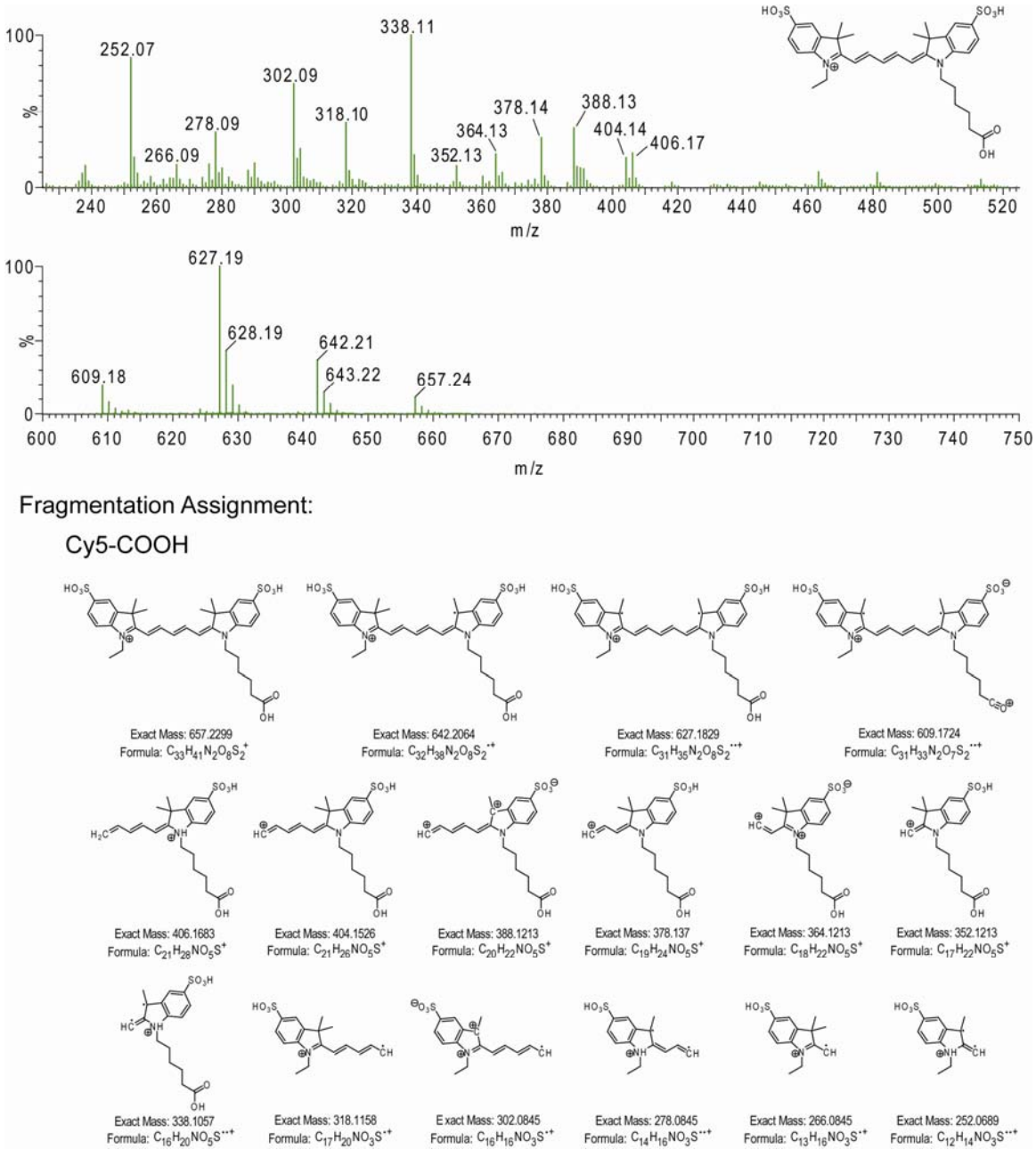

Figure S5. Positive mode MS/MS and peak assignment of the Cy5-COOH starting material. The mass value, chemical formula, and a possible structure are shown for each major peak in the MS/MS spectrum. Given the high degree of conjugation of the system, other resonance forms or bond rearrangements for these structures may also account for these peaks, but are omitted for clarity.

Figure S6

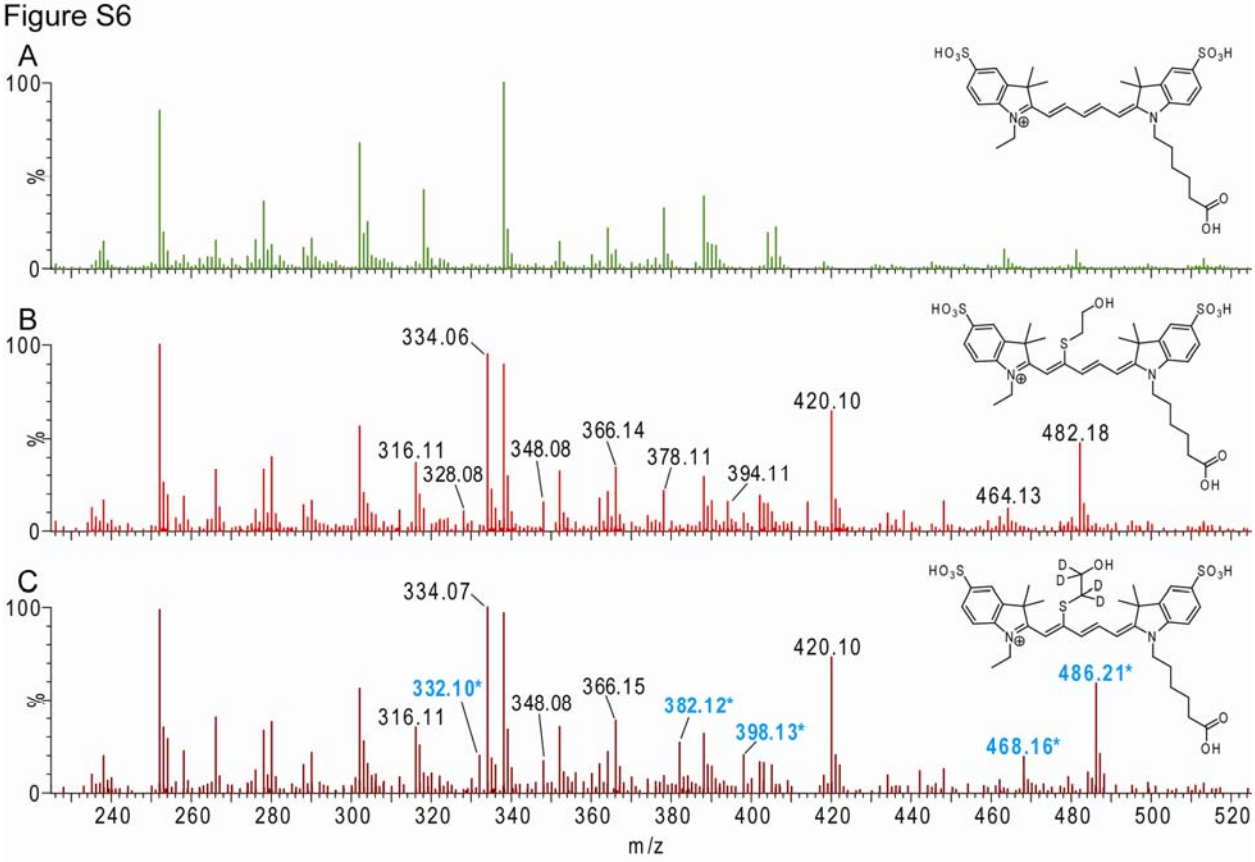

Fragmentation Assignment:

Cy5-COOH-βME dark state

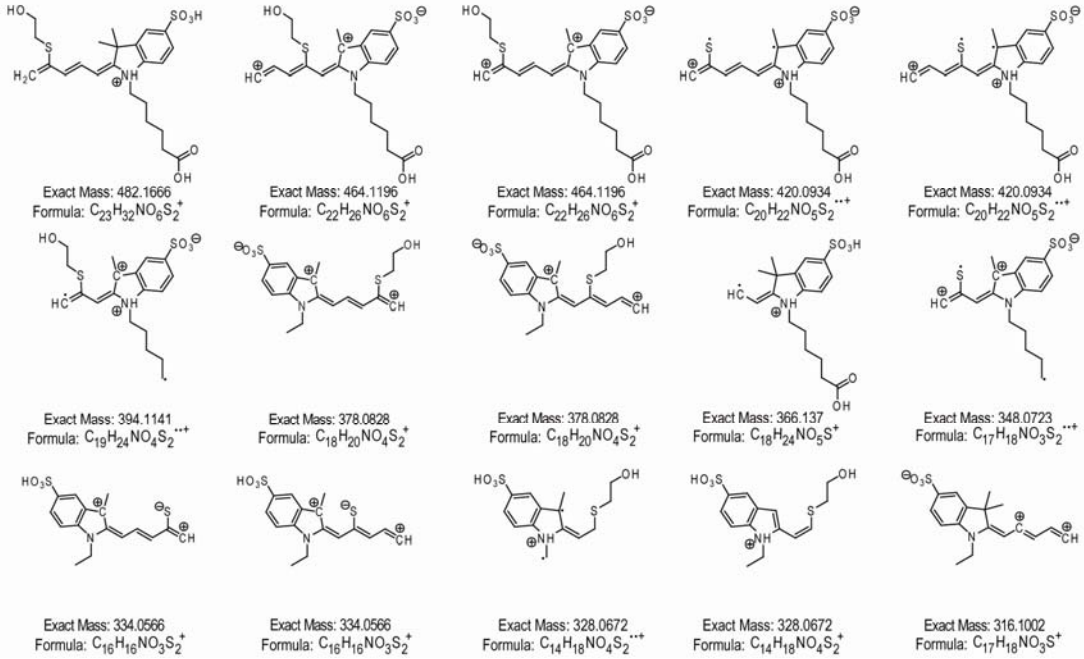

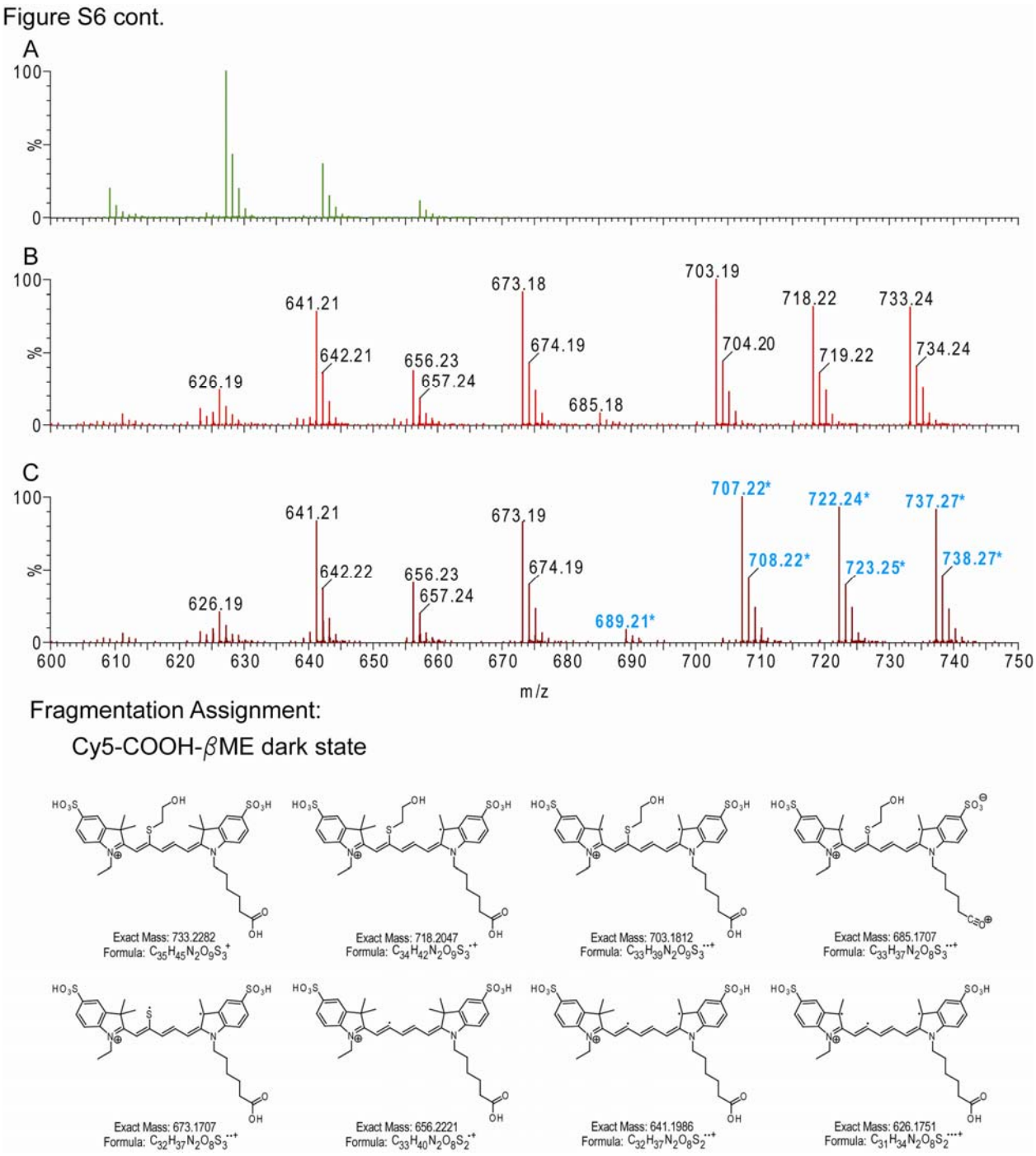

Figure S6. Positive mode MS/MS and peak assignment of the Cy5-COOH-βME conjugate. Fragmentation pattern of the starting material Cy5-COOH (A), dark state product generated in the presence of βME (B), and dark state product generated with deuterated d_4-βME (C) are shown in the upper three panels. The expected structures of the parent ions are drawn in the

upper right portion of each panel, with D representing the replacement of hydrogen with deuterium. All peaks observed for the starting Cy5-COOH material were also observed in the dark state samples, with 1-Dalton shift in certain cases due to oxidation. The additional peaks that were observed for the dark state product, but not for the starting material, are highlighted by presenting their |*m/*z| values. Peaks (highlighted in cyan with an asterisk) in which the thiol remains intact during fragmentation show a 4-Dalton shift when d_4-βME instead of βME was used to generate the dark state product. Below the spectrum, the mass value, chemical formula, and a possible structure are shown for each major peak in the MS/MS spectrum. Again, other resonance forms or bond rearrangements for these structures may also exist, but are omitted for clarity.

Figure S7

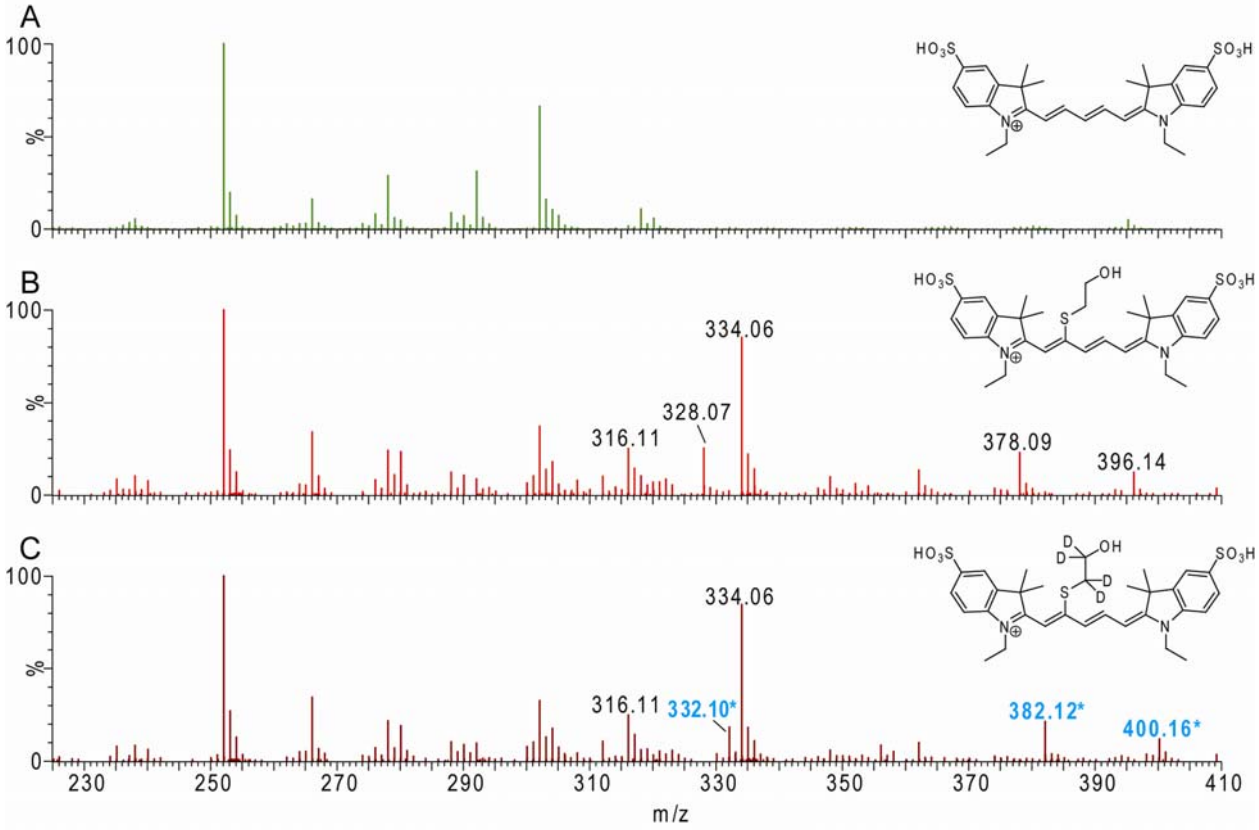

Fragmentation Assignment:

Cy5-diethyl-βME dark state

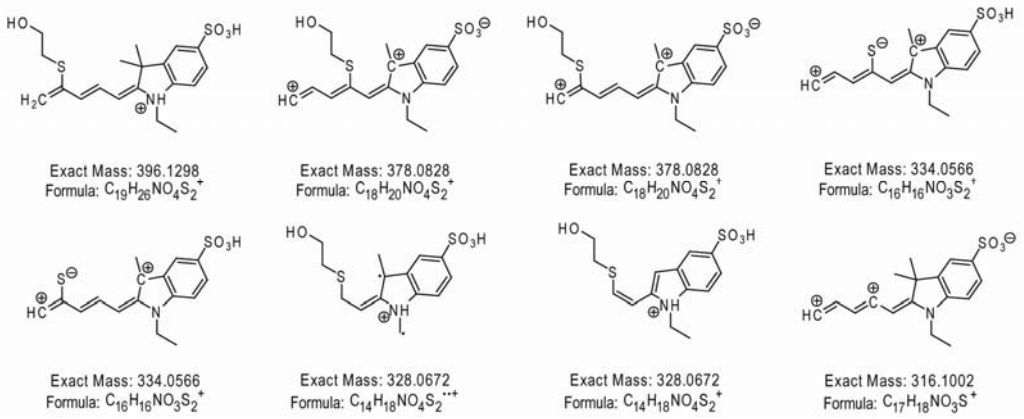

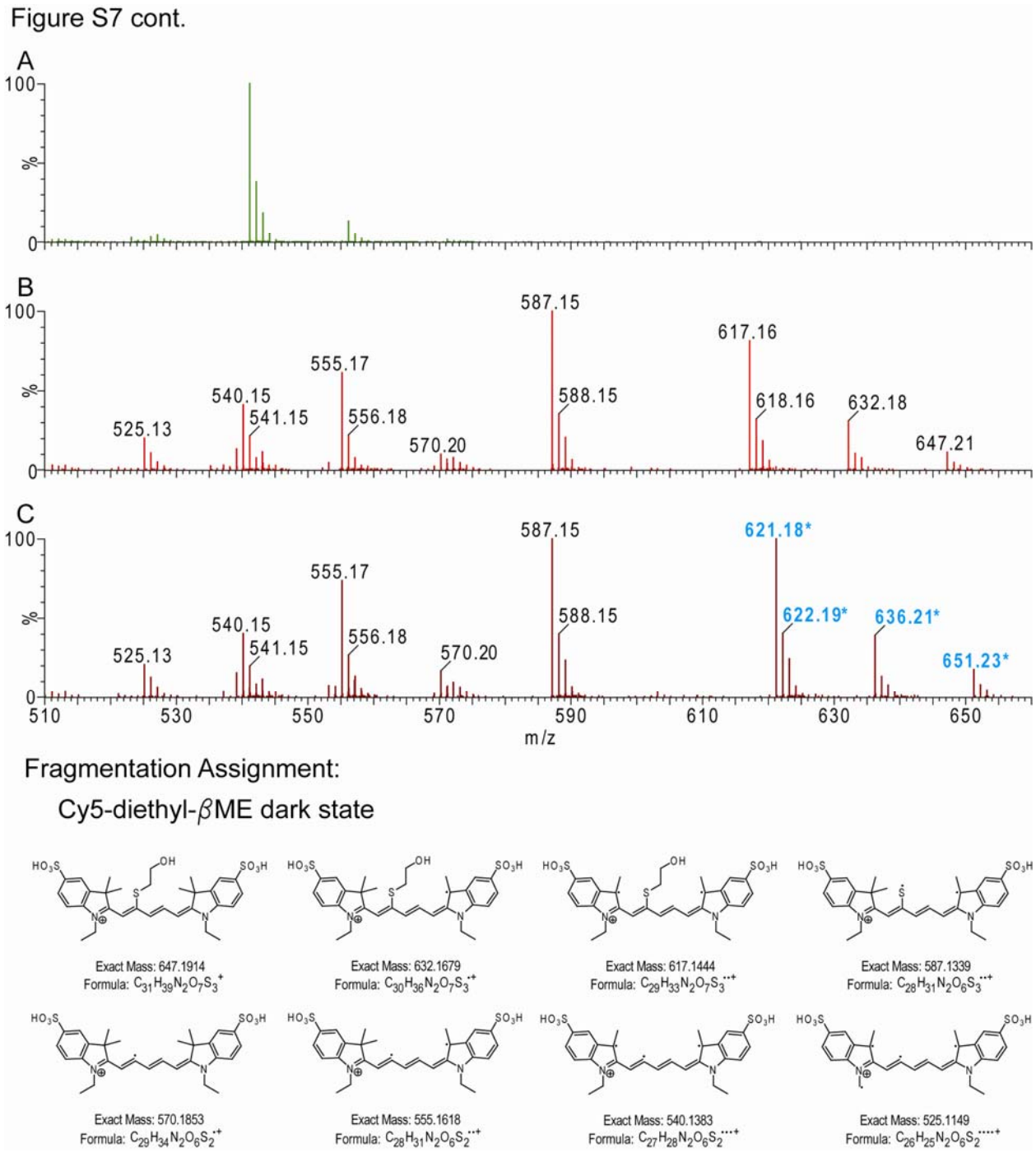

Figure S7. Positive mode MS/MS of Cy5-diethyl and its βME conjugate. Fragmentation pattern of the starting material Cy5-diethyl (A), dark state generated in the presence of βME (B), and dark state generated with d_4-βME (C) are presented in the upper three panels. The expected structures of the parent ions are drawn in the upper right portion of each panel, with D

representing the replacement of hydrogen with deuterium. All peaks observed for the starting Cy5-diethyl material were also observed in the dark state case, with 1-Dalton shift in certain cases due to oxidation. The additional peaks that were observed for the dark state product, but not for the starting material, are highlighted by presenting their $|m/z|$ values. Peaks (highlighted in cyan with an asterisk) in which the thiol remains intact during fragmentation show a 4-Dalton shift when d_4-βME instead of βME was used to generated the dark state product. As in Figures S5 and S6, the mass value, chemical formula, and a possible structure are shown for each major peak in the MS/MS spectrum. Other resonance forms or bond rearrangements for these structures may also exist, but are omitted for clarity.

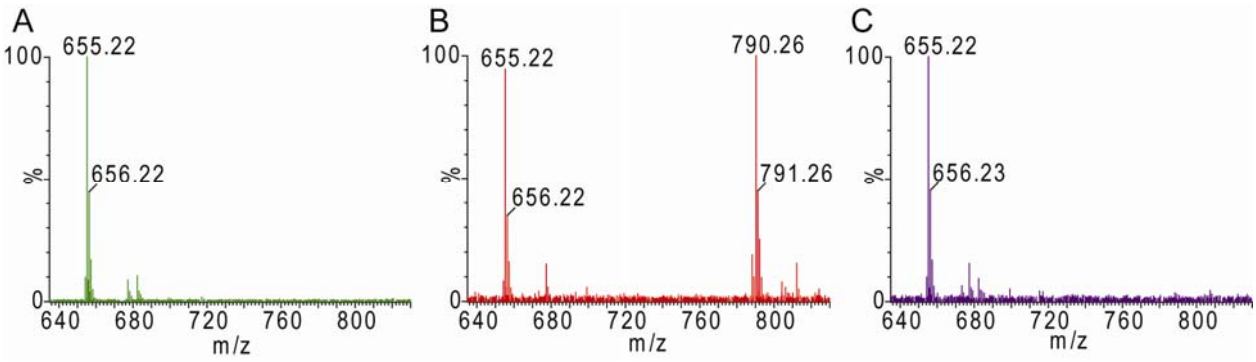

Figure S8. Negative mode MS of the dark state of Cy5-COOH formed in the presence of L-Cys-ME. The panels show the cyanine dye-thiol mixture before (A) and after (B) red laser illumination, as well as after reactivation (C) by UV excitation. The peak that appears at $[M-2H]^-$ $|m/z| = 655.22$ corresponds to $[Cy5\text{-}COO]^-$. After red illumination, a new peak emerges as a singly charged species at $[M-H]^-$ $|m/z| = 790.26$. After UV illumination to recover the dye to the fluorescent state, the new peak disappears, indicating that the peak indeed corresponds to the photoconversion product.

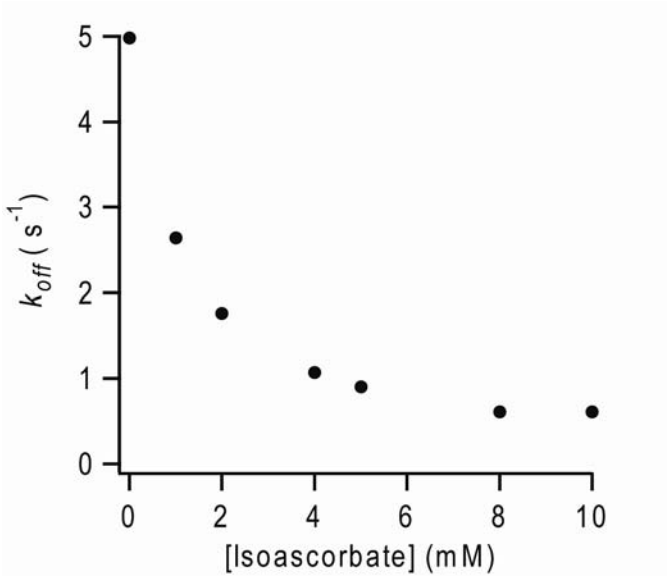

Figure S9. Effect of radical quencher on Cy5 switching kinetics. The switching rate to the dark state was measured for single Cy5 molecules in the presence of 10 mM MEA and varied concentrations of the radical quencher, sodium D-isoascorbate.

Table S1. Predicted and measured masses, in the negative ionization mode, of cyanine dyes and their corresponding dark state products shown in Scheme 2. Since both the original dye molecules and the dark state products detected by ESI-LC/MS exhibit a single negative charge, the expected *m/z* values were calculated from the singly charged forms of cyanine dyes and corresponding dark state products.

Thiol	Cyanine dye	Predicted cyanine dye $[M-2H]^-$ |*m/z*|	Observed cyanine dye $[M-2H]^-$ |*m/z*|	Predicted dark state $[M-H]^-$ |*m/z*|	Observed dark state $[M-H]^-$ |*m/z*|
βME	Cy5-COOH	655.2153	655.2117	733.2293	733.2242
L-Cys-ME	Cy5-COOH	655.2153	655.2158	790.2507	790.2560
MEA	Cy5-COOH	655.2153	655.2126	732.2453	732.2407
βME	Cy5-diethyl	569.1786	569.1736	647.1925	647.1931
L-Cys-ME	Cy5-diethyl	569.1786	569.1746	704.2140	704.2167
MEA	Cy5-diethyl	569.1786	569.1746	646.2085	646.2070
MEA	Cy7-COOH	681.2310	681.2310	758.2609	758.2668

References:

(1) Bates, M.; Huang, B.; Dempsey, G. T.; Zhuang, X. *Science* **2007**, *317*, 1749-1753.

(2) Bates, M.; Blosser, T. R.; Zhuang, X. *Phys. Rev. Lett* **2005**, *94*, 108101.

(3) Lang, W.; Caldwell, G. W.; Li, J.; Leo, G. C.; Jones, W. J.; Masucci, J. A. *Drug Metab Dispos* **2007**, *35*, 21-9.

(4) Parshikov, I. A.; Freeman, J. P.; Lay, J. O., Jr.; Beger, R. D.; Williams, A. J.; Sutherland, J. B. *Appl Environ Microbiol* **2000**, *66*, 2664-7.

(5) Cole, R. B. *J. Mass Spec.* **2000**, 35, 763-772.

(6) Vessecchi, R.; Crotti, A. E. M.; Guaratini, T.; Colepicolo, P.; Galembeck, S. E.; Lopes, N. P. *Mini-Rev. Org. Chem.* **2007**, 4, 75-87.